Molecular Therapy
Oncolytics
Original Article

AMERICAN SOCIETY of GENE & CELL THERAPY

miR-424-5p Promotes Anoikis Resistance and Lung Metastasis by Inactivating Hippo Signaling in Thyroid Cancer

Xiaoli Liu,[1] Yantao Fu,[1] Guang Zhang,[1] Daqi Zhang,[1] Nan Liang,[1] Fang Li,[1] Changlin Li,[1] Chengqiu Sui,[1] Jinxi Jiang,[1] Hongzhi Lu,[1] Zihan Zhao,[1] Gianlorenzo Dionigi,[2] and Hui Sun[1]

[1]Division of Thyroid Surgery, China-Japan Union Hospital of Jilin University, Jilin Provincial Key Laboratory of Surgical Translational Medicine, Changchun City, Jilin Province, 130033, China; [2]Division for Endocrine and Minimally Invasive Surgery, Department of Human Pathology in Adulthood and Childhood "G. Barresi," University Hospital "G. Martino," University of Messina, Messina, Italy

miR-424-5p has been widely identified to function as an oncomiR in multiple human cancer types. However, the biological function of miR-424-5p in distant metastasis of thyroid cancer, as well as the underlying mechanism, remains not clarified yet. In the current study, miR-424-5p expression was elucidated in 10 paired fresh thyroid cancer tissues and the thyroid cancer dataset from The Cancer Genome Atlas (TCGA). Lung metastasis colonization models *in vivo* and functional assays *in vitro* were used to determine the role of miR-424-5p in thyroid cancer. Bioinformatics analysis, western blot, luciferase reporter, and immunofluorescence assays were applied to identify the potential targets and underlying mechanism involved in the functional role of miR-424-5p in lung metastasis of thyroid cancer. Here, we reported that miR-424-5p was upregulated in thyroid cancer, and overexpression of miR-424-5p significantly correlated with distant metastasis of thyroid cancer. Upregulating miR-424-5p promoted, whereas silencing miR-424-5p inhibited, anoikis resistance *in vitro* and lung metastasis *in vivo*. Mechanistic investigation further revealed that miR-424-5p promoted anoikis resistance and lung metastasis by inactivating Hippo signaling via simultaneously targeting WWC1, SAV1, and LAST2. Therefore, our results support the idea that miR-424-5p may serve as a potential therapeutic target in lung metastasis of thyroid cancer.

INTRODUCTION

Thyroid cancer is one of the most prevalent endocrine malignancies, with an increasing incidence in recent years worldwide.[1,2] Based on substantial progresses in the treatment of thyroid cancer, the vast majority of thyroid cancer patients have an excellent prognosis, with a 5-year survival rate exceeding 95%.[3] However, early metastasis of the malignancy to distant organ is a critical contributor affecting the prognosis of thyroid cancer patients.[4] Among the metastatic sites of thyroid cancer, lung is the most frequently seen distant metastatic organ due to high hemodynamics.[5] Therefore, identification of novel therapeutic strategies to reduce the incidence of lung metastasis will achieve long-term remission in thyroid cancer patients.

As a tumor-suppressive signaling, the Hippo signaling has been frequently identified to be inactivated in distinct human cancer types.[6–8] Primarily four protein components, including kinases MST1/2 and LATS1/2 and adaptor proteins SAV1 and MOB1, constitute core kinase cassette of the Hippo pathway.[8] By tightly balancing the activity of YAP and TAZ through phosphorylation-ubiquitination mechanisms, the Hippo signaling keeps constitutively active.[9,10] By contrast, unphosphorylated YAP1/TAZ translocates to the nucleus of cells and induces the transcriptional activity of TEA domain (TEAD) family members as the transcriptional co-activators when Hippo signaling is inactive, which further transcriptionally upregulates multiple downstream effectors to exert a pleiotropic role in progression and metastasis of cancers.[11,12] Garcia-Rendueles et al.[13] have shown that NF2 loss promoted RAS-induced thyroid cancers via inactivating Hippo signaling. And importantly, inactivation of Hippo signaling predicted poor prognosis in thyroid cancer patients.[14] These studies suggest that identification of the underlying mechanism responsible for inactivation of the Hippo pathway will improve the prognosis of thyroid cancer patients.

MicroRNAs (miRNAs) are a class of endogenous non-coding RNAs. miRNAs post-transcriptionally regulate gene expression via interacting with the 3′ UTR of downstream target genes.[15] miRNAs exert their functions in several biological processes, including cell differentiation, proliferation, and cardiogenesis.[15,16] Aberrant expressions of miRNAs are implicated in the development, progression, and metastasis in a variety of cancers.[17–24] Furthermore, deregulation of miRNA expression significantly contributes to the tumorigenesis and metastasis of thyroid neoplasias.[25] miR-424-5p, one of the originally discovered miRNAs, has been identified to be upregulated in multiple human cancer types.[26–28] Our preliminary study has

Received 10 June 2019; accepted 28 October 2019;
https://doi.org/10.1016/j.omto.2019.10.008.

Correspondence: Hui Sun, Division of Thyroid Surgery, China-Japan Union Hospital of Jilin University, Jilin Provincial Key Laboratory of Surgical Translational Medicine, Changchun City, Jilin Province, 130033, China.
E-mail: thyroidjl@163.com

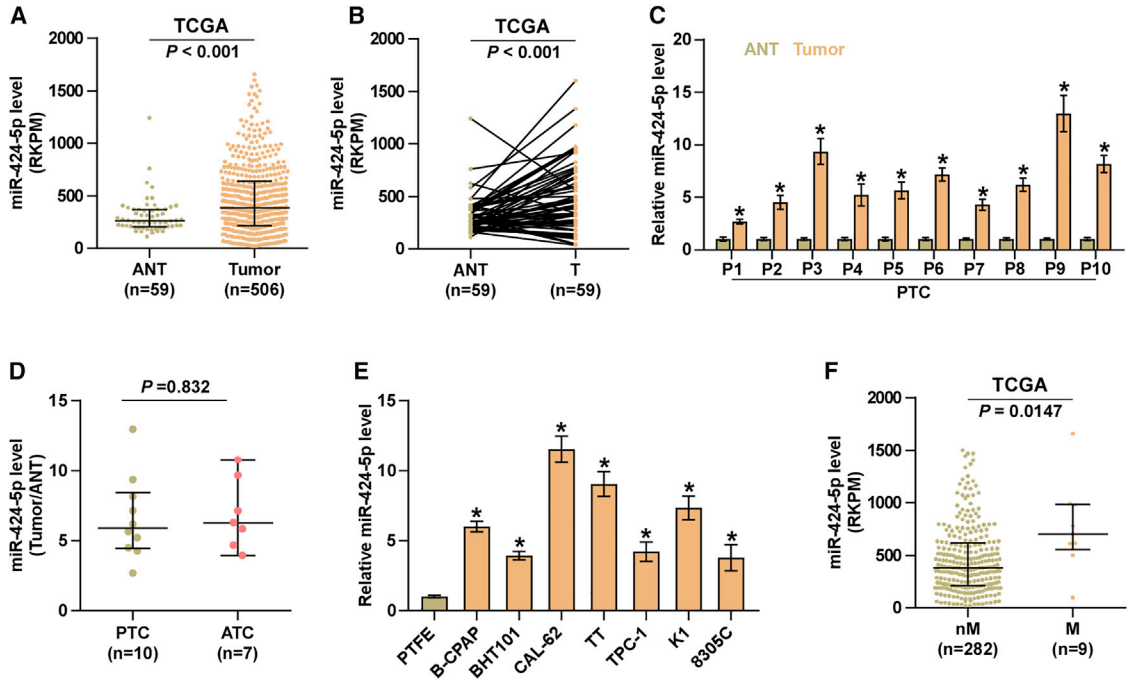

Figure 1. miR-424-5p Expression Is Elevated in Thyroid Cancer

(A) miR-424-5p expression level in thyroid cancer tissues and the adjacent normal tissues (ANTs) as assessed by analyzing the RNA sequencing dataset of thyroid cancer from TCGA (ANT, n = 59; thyroid cancer, n = 505). Each bar represents the median values ± quartile values. (B) miR-424-5p expression level in 59 paired thyroid cancer tissues and the matched adjacent normal tissues as assessed by analyzing the RNA sequencing dataset of thyroid cancer from TCGA. (C) Real-time PCR analysis of miR-424-5p expression in 10 fresh paired thyroid cancer tissues. GAPDH was used as endogenous controls. Each bar represents the mean values ± SD of three independent experiments. *p < 0.05. (D) miR-424-5p expression level examined in 10 papillary thyroid cancer tissues and 7 anaplastic thyroid cancer tissues. Each bar represents the median values ± quartile values. (E) Real-time PCR analysis of miR-424-5p expression in normal thyroid follicular epithelial cells, PTFE cells, and seven thyroid cancer cells, including four papillary thyroid cancer (PTC) cell lines (B-CPAP, BHT101, TPC-1, and K1), two anaplastic thyroid cancer (ATC) cell lines (CAL-62 and 8305C), and one thyroid duct cell carcinoma cells, TT. GAPDH was used as endogenous controls. Each bar represents the mean values ± SD of three independent experiments. *p < 0.05. (F) miR-424-5p expression level in metastatic thyroid cancer tissues (M, n = 9) and non-metastatic thyroid cancer tissues (nM, n = 282) by analyzing the RNA sequencing dataset of thyroid cancer from TCGA. Each bar represents the median values ± quartile values.

revealed that miR-424-5p was upregulated in thyroid cancer tissues, which was positively associated with aggressive clinical features in thyroid cancer patients,[29] suggesting that miR-424-5p may play an important role in malignant progression or metastasis of thyroid cancer patients. However, the clinical significance and functional roles of miR-424-5p in thyroid cancer, particularly in the metastasis of thyroid cancer, remain not yet elucidated.

In the current study, our findings demonstrated that miR-424-5p was overexpressed in thyroid cancer tissues, which was positively associated with distant metastasis of thyroid cancer. Our findings further showed that upregulating of miR-424-5p promoted anoikis resistance and lung metastasis of thyroid cancer cells *in vitro* and *in vivo*. Conversely, silencing miR-424-5p yielded an opposite effect on lung metastasis of thyroid cancer. Moreover, we found that miR-424-5p inhibited activity of Hippo signaling via directly targeting WWC1, SAV1, and LAST2, which further promoted anoikis resistance and lung metastasis in thyroid cancer. Therefore, our findings determine that miR-424-5p plays an important role in lung metastasis of thyroid cancer.

RESULTS

miR-424-5p Is Upregulated in Thyroid Cancer

To evaluate miR-424-5p expression in thyroid cancer, we analyzed an miRNAs dataset of thyroid cancer from The Cancer Genome Atlas (TCGA), and the results showed that miR-424-5p was remarkably upregulated in thyroid cancer tissues compared with the adjacent normal tissues (ANTs) (Figure 1A). Consistently, expression levels of miR-424-5p in 59 paired thyroid cancer tissues were dramatically overexpressed compared with those in the matched ANTs in the majority of thyroid cancer tissues (Figure 1B), which was further demonstrated in our 10 paired thyroid cancer tissues (Figure 1C). However, there was no significant difference of miR-424-5p expression in 10 papillary thyroid cancer (PTC) samples and 7 anaplastic thyroid cancer (ATC) samples (Figure 1D). The expression levels of miR-424-5p in normal thyroid follicular epithelial cells, primary thyroid follicular epithelial (PTFE) cells, and seven thyroid cancer cells, including one thyroid duct cell carcinoma cell TT, two anaplastic thyroid cancer cell lines, CAL-62 and 8305C, and four papillary thyroid cancer cell lines, B-CPAP, BHT101, TPC-1, and K1. As shown in Figure 1E, we found that miR-424-5p expression in thyroid cancer cells

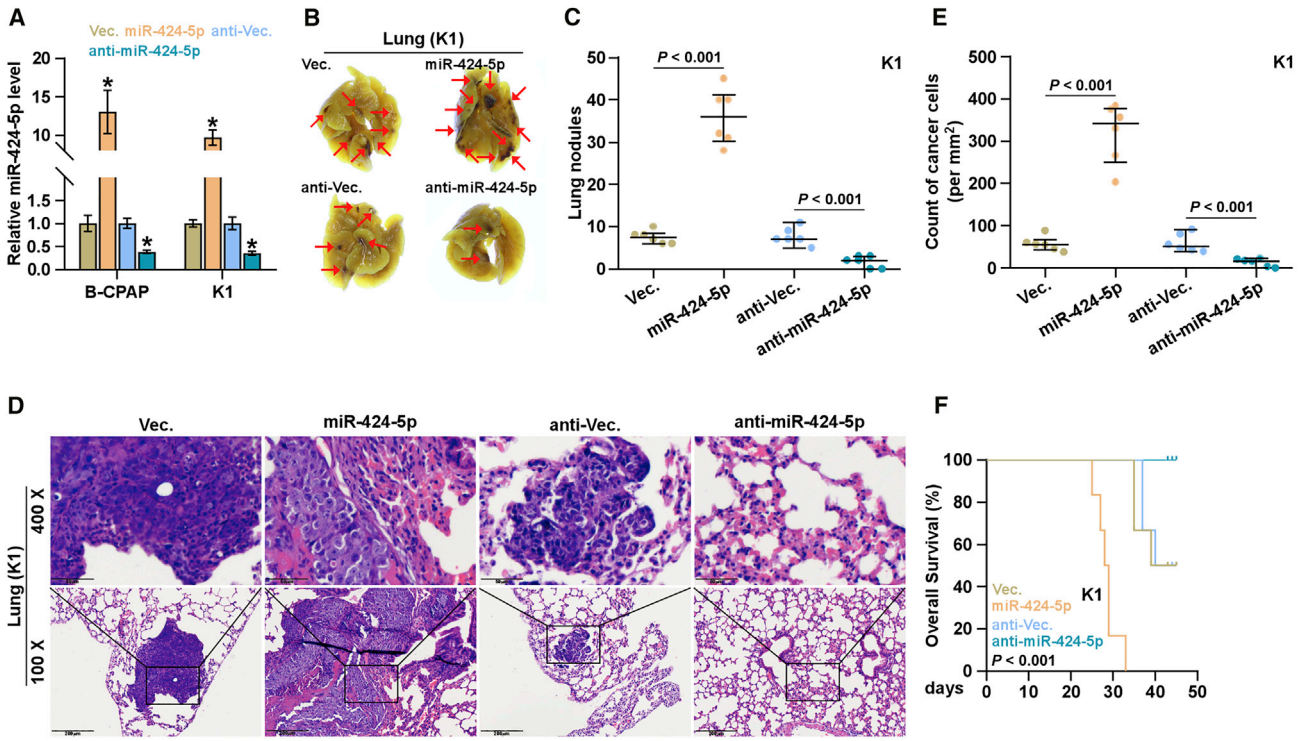

Figure 2. Silencing miR-424-5p Suppresses Lung Metastasis of Thyroid Cancer Cells *In Vivo*

(A) Real-time PCR analysis of miR-424-5p expression in the vector, miR-424-5p-overexpressing, anti-vector, and miR-424-5p-downexpressing thyroid cancer cells. Error bars represent the mean ± s.d. of three independent experiments. *p < 0.05. (B) Representative images of the lung metastases formed from the indicated cells in the mice (n = 6, each group). (C) The numbers of lung tumor nests in each group were counted under a low-power field and are presented as the median values ± quartile values (right panel). *p < 0.05. Each bar represents the median values ± quartile values. (D) Representative H&E staining images of lung metastasis nodules in the indicated mouse groups. Scale bars, 200 μm (original magnification ×100); 50 μm (original magnification ×400). (E) The quantification of the number of thyroid cancer cells (/mm^2) in the indicated tumor tissues. Error bars represent the mean ± SD values. *p < 0.05. (F) Kaplan-Meier survival curves from the indicated mouse groups.

was differentially upregulated compared with that in PTFE cells. Importantly, miR-424-5p expression was observed to be significantly upregulated in thyroid cancer tissues with distant organ metastasis compared with that without metastasis via analyzing a thyroid cancer dataset from TCGA (Figure 1F). Collectively, these results indicated that miR-424-5p is upregulated in thyroid cancer, which may be implicated in distant metastasis of thyroid cancer.

miR-424-5p Promotes Lung Metastasis of Thyroid Cancer

Because lung has been reported to be the most common distant metastatic organ among all metastatic sites of thyroid cancer,[5] the effect of miR-424-5p on lung metastasis of thyroid cancer was first investigated in lung colonization models *in vivo*. We further established miR-424-5p stably expressing B-CPAP and K1 cell lines by ectopically overexpressing miR-424-5p and endogenously knocking down miR-424-5p via retrovirus infection (Figure 2A). Vector, miR-424-5p-overexpressing, or anti-miR-424-5p K1 cells were injected into the mice via tail veins, respectively. As shown in Figures 2B and 2C, upregulating miR-424-5p enhanced the number of lung metastatic nodules. H&E staining revealed that upregulating miR-424-5p increased the lung metastasis burden of K1 cells (Figure 2D). Furthermore, upregulating miR-424-5p dramatically elevated the number of cancer cells per square millimeter (Figure 2E), as well as reduced the overall survival of the mice (Figure 2F). Conversely, silencing miR-424-5p yielded a dramatically opposite role in lung metastasis of thyroid cancer (Figures 2A–2F). Taken together, our results demonstrated that miR-424-5p promotes lung metastasis ability of thyroid cancer cells *in vivo*.

Proliferation of Thyroid Cancer Cells Is Not Impeded by miR-424-5p *In Vitro*

We further investigated the functional role of miR-424-5p in lung metastasis of thyroid cancer. Cell Counting Kit-8 (CCK-8) assay was first performed to examine the effect of miR-424-5p on thyroid cancer cells, and the result showed that silencing miR-424-5p slightly inhibited the cell growth of B-CPAP and K1 cells; however, upregulating miR-424-5p had no effect on cell proliferation of thyroid cancer cells (Figures 3A–3D). Furthermore, neither colony formation ability nor cell-cycle progression in thyroid cancer cells was affected by changed expression of miR-424-5p (Figures 3E and 3F). Furthermore, we found that either upregulating or downregulating miR-424-5p had no significant effect on tumor growth of thyroid cancer cells *in vivo* (Figures 3G–3I). However, upregulating miR-424-5p promoted, whereas silencing miR-424-5p repressed, anchorage-independent

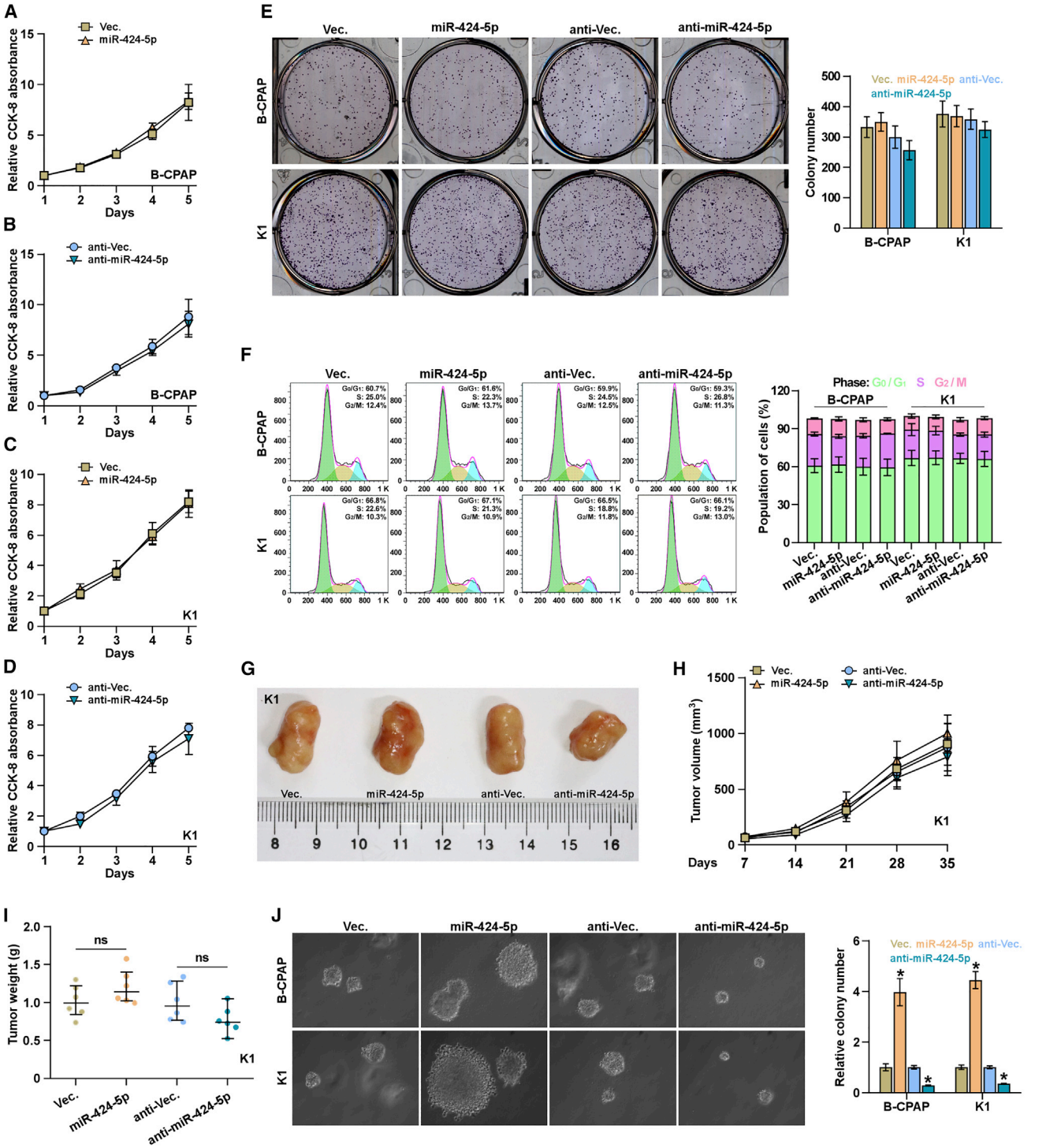

Figure 3. miR-424-5p Does Not Affect Growth and Proliferation of Thyroid Cancer Cells

The effects of miR-424-5p on proliferation rate in the indicated B-CPAP (A and B) and K1 (C and D) cells via CCK-8 assay. Each bar represents the mean values ± SD of three independent experiments. (E) The effects of miR-424-5p on colony formation ability in the indicated thyroid cancer cells via colony formation assay. Each bar represents the mean values ± SD of three independent experiments. (F) Flow cytometric analysis of the effects of miR-424-5p on cell cycle in the indicated thyroid cancer cells. Each bar represents the mean values ± SD of three independent experiments. (G) Images of excised tumors from the mice at 35 days

(legend continued on next page)

growth capability of thyroid cancer cells (Figure 3J). Therefore, these results indicated that miR-424-5p does not impede the proliferation ability of thyroid cancer cells *in vitro*.

miR-424-5p Promotes Anoikis Resistance, Invasion, and Migration

As demonstrated above, upregulating miR-424-5p significantly augmented anchorage-independent growth capability of thyroid cancer cells. Several lines of evidence have reported that anoikis resistance, namely, the capacity of cancer cells to survive under suspension conditions, is a major hallmark of metastatic cancer cells, which significantly contributes to distant metastasis in a variety of cancers.[30–32] Therefore, the effect of miR-424-5p on anoikis resistance of thyroid cancer cells was further investigated. As shown in Figure 4A, upregulating miR-424-5p reduced the apoptosis rate of thyroid cancer cells; however, silencing miR-424-5p elevated the apoptosis rate in thyroid cancer cells. Moreover, upregulating miR-424-5p increased, whereas silencing miR-424-5p lowered, the mitochondrial potential of thyroid cancer cells via mitochondrial membrane potential assay (Figure 4B). Then, we further examined the effects of miR-424-5p on the activity caspase-3 and -9, and the expression of anti-apoptotic protein, BCL2 and BCL2L1, and pro-apoptotic protein, BAX and BAD, in thyroid cancer cells, and found that overexpression of miR-424-5p increased BCL2 and BCL2L1 expression, reduced BAX and BAD expression, and repressed the activity of caspase-3 or -9 in thyroid cancer cells (Figures 4C–4E). By contrast, silencing miR-424-5p displayed an opposite effect (Figures 4C–4E). Furthermore, upregulating miR-424-5p enhanced, whereas silencing miR-424-5p inhibited, invasion and migration abilities of thyroid cancer cells (Figures 4F and 4G). Collectively, these results revealed that miR-424-5p promotes anoikis resistance, invasion, and migration in thyroid cancer cells.

miR-424-5p Inactivates the Hippo Signaling Pathway

To determine the underlying mechanism involved in a pro-lung metastasis role of miR-424-5p in thyroid cancer, luciferase reporter plasmids of multiple signaling pathways were transfected into thyroid cancer cells, respectively, and we found that transcriptional activity of TEAD, the transcriptional co-activators of the Hippo signaling pathway, was inactivated by miR-424-5p overexpression, but silenced by silencing miR-424-5p in thyroid cancer cells (Figures 5A and 5B). Immunofluorescence assay showed that upregulating miR-424-5p promoted, whereas silencing miR-424-5p reduced, nuclear translocation of YAP in thyroid cancer cells (Figure 5C). Real-time PCR analysis showed that upregulating miR-424-5p inhibited, whereas silencing miR-424-5p upregulated, expression levels of multiple downstream genes, including CTGF, CYR61, SOX9, and HOXA1, of the Hippo pathway in thyroid cancer cells (Figures 5D and 5E). Thus, these findings indicated that miR-424-5p represses activity of Hippo signaling in thyroid cancer.

miR-424-5p Targets WWC1, SAV1, and LAST2

By analyzing several available algorithms, including TargetScan (http://www.targetscan.org/vert_71/),[33] miRanda (http://www.microrna.org/microrna/microrna/home.do),[34] and miRWalk (http://zmf.umm.uni-heidelberg.de/apps/zmf/mirwalk/),[35] we found that multiple core components of Hippo signaling, including WWC1, SAV1, and LAST2, may be the potential targets of miR-424-5p (Figure 6A). Western blotting analysis revealed that upregulating miR-424-5p repressed WWC1, SAV1, and LAST2 expression, and meanwhile reduced phosphorylated MST1/2, LATS1, and YAP levels and increased nuclear YAP and TAZ expression, but had no effect on total level of MST1 and LATS1 in thyroid cancer cells (Figure 6B). By contrast, silencing miR-424-5p presented an opposite pattern (Figure 6B). RNA immunoprecipitation (IP) assay revealed a direct association of miR-424-5p with the transcripts of WWC1, SAV1, and LAST2 (Figures 6C and 6D). Furthermore, luciferase assay demonstrated that upregulating miR-424-5p suppressed, whereas silencing miR-424-5p increased, the reporter activity of 3′ UTR of WWC1, SAV1, and LAST2, but not of the mutant 3′ UTR of WWC1, SAV1, and LAST2 (Figures 6E and 6F). Therefore, our results demonstrated that WWC1, SAV1, and LAST2 are direct targets of miR-424-5p in thyroid cancer cells.

miR-424-5p Promotes Anoikis Resistance and Lung Metastasis via Inactivating Hippo Signaling

To investigate the functional role of Hippo signaling in miR-424-5p-induced anoikis resistance of thyroid cancer cells, we further applied a constitutively activating YAP1,[36] YAP1-S127A, in miR-424-5p-silenced thyroid cancer cells, and found that YAP1-S127A dramatically reversed the HOP-Flash activity repressed by downregulation of miR-424-5p (Figure 7A). The pro-apoptotic role of miR-424-5p downexpression in thyroid cancer, as well as the inhibitory effect of miR-424-5p downexpression on mitochondrial potential and anchorage-independent growth capability, was significantly reversed by YAP1-S127A (Figures 7B–7D). Furthermore, silencing YAP1 reduced the anchorage-independent growth induced by miR424-5p overexpression in thyroid cancer cells (Figure 7E). Importantly, silencing YAP1 remarkably repressed the lung metastatic ability in miR-424-5p-overexpressing thyroid cancer cells *in vivo*. Conversely, overexpressing YAP1 reversed the inhibitory effects of anti-miR-424-5p in lung metastasis of thyroid cancer cells *in vivo* (Figures 7F–7H). Taken together, our results indicated that miR-424-5p promotes anoikis resistance and lung metastasis via inactivating Hippo signaling in thyroid cancer.

miR-424-5p Negatively Correlates with WWC1, SAV1 and LAST2, and YAP1

As shown in Figures S1A and S1B, miR-424-5p expression was increased in clinical thyroid cancer tissues; conversely, WWC1, SAV1 and LAST2, and YAP1 expression levels were differentially

after injection with the indicated cells. (H) Tumor volumes were measured every 5 days. Each bar represents the median values ± quartile values. (I) Average weight of excised tumors from the indicated mice. Each bar represents the median values ± quartile values. (J) The effects of miR-424-5p on anchorage-independent ability in the indicated thyroid cancer cells via anchorage-independent growth assay. Each bar represents the mean values ± SD of three independent experiments. $^{*}p < 0.05$.

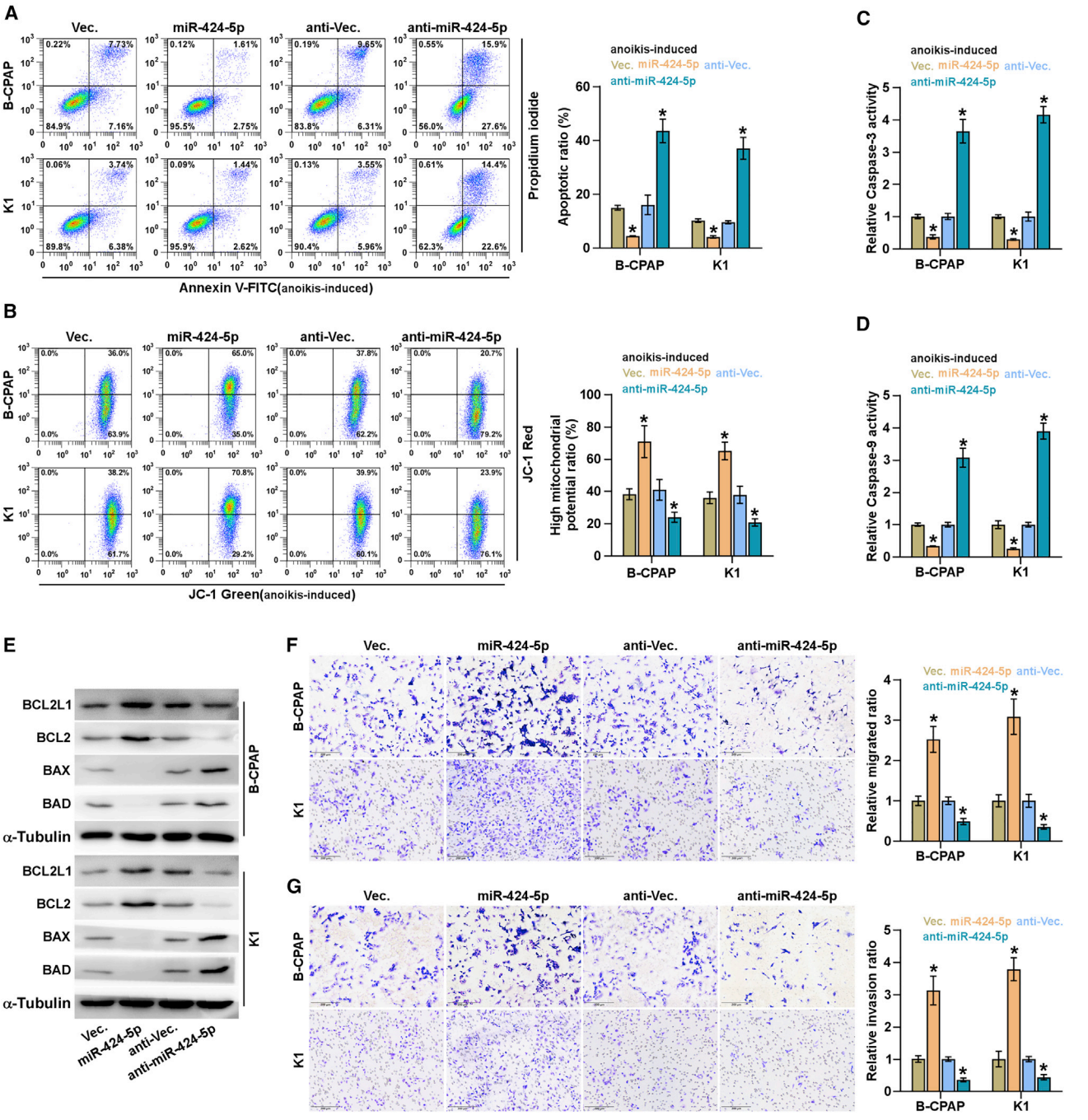

Figure 4. miR-424-5p Promotes Anoikis Resistance in Thyroid Cancer Cells

(A) The effects of miR-424-5p on apoptotic ratio in the indicated thyroid cancer cells via annexin V-FITC/PI staining. Error bars represent the mean ± SD of three independent experiments. (B) The effects of miR-424-5p on mitochondrial potential in the indicated thyroid cancer cells via JC-1 staining assay. Error bars represent the mean ± SD of three independent experiments. (C and D) Analyses of the activities of caspase-3 (C) and caspase-9 (D) were detected by the cleaved forms of these two proteins. Error bars represent the mean ± SD of three independent experiments. (E) Western blotting analysis of BAX, BAD, BCL2L1, and BCL2 expression in the indicated thyroid cancer cells. α-Tubulin served as the loading control. (F and G) The effects of miR-424-5p on migration (F) and invasion (G) ability in the indicated thyroid cancer cells. Error bars represent the mean ± SD of three independent experiments. *$p < 0.05$.

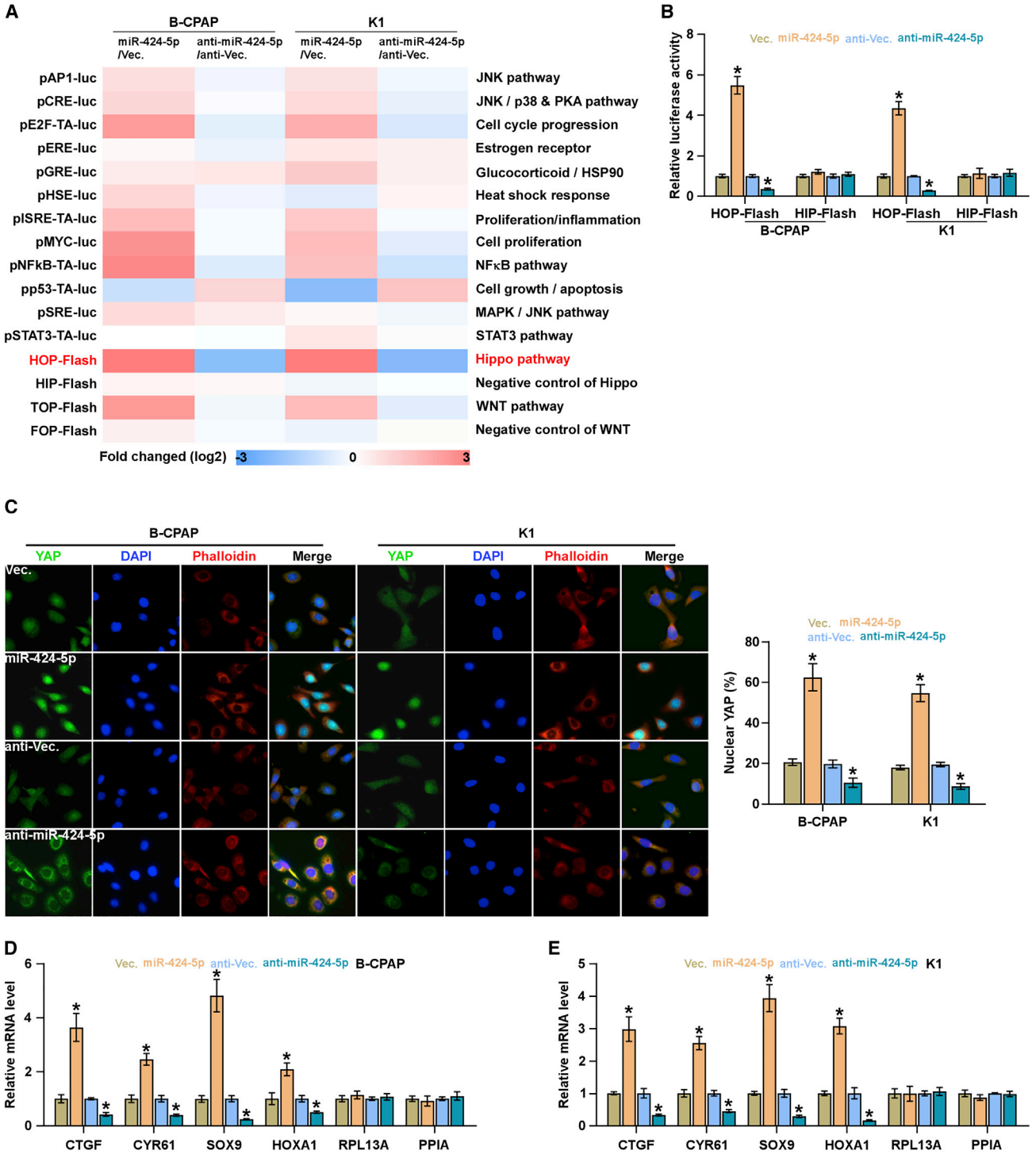

Figure 5. miR-424-5p Inhibits Activity of the Hippo Signaling Pathway

(A) Activity of luciferase reporter constructs of several signaling pathways was examined in the miR-424-5p-overexpressing or -silencing thyroid cancer cells. (B) TEAD transcriptional activity was assessed by HOP-Flash luciferase reporter in the indicated cells. Error bars represent the mean ± SD of three independent experiments. (C) Representative immunofluorescent images of the indicated thyroid cancer cells immunostained with YAP antibody (red), phalloidin (green), or DAPI (blue). Each bar represents the mean values ± SD of three independent experiments. (D and E) Real-time PCR analysis of CTGF, CYR61, SOX9, HOXA1, RPL13A, and PPIA in the B-CPAP (D) and K1 (E) cells. Error bars represent the mean ± SD of three independent experiments. *p < 0.05.

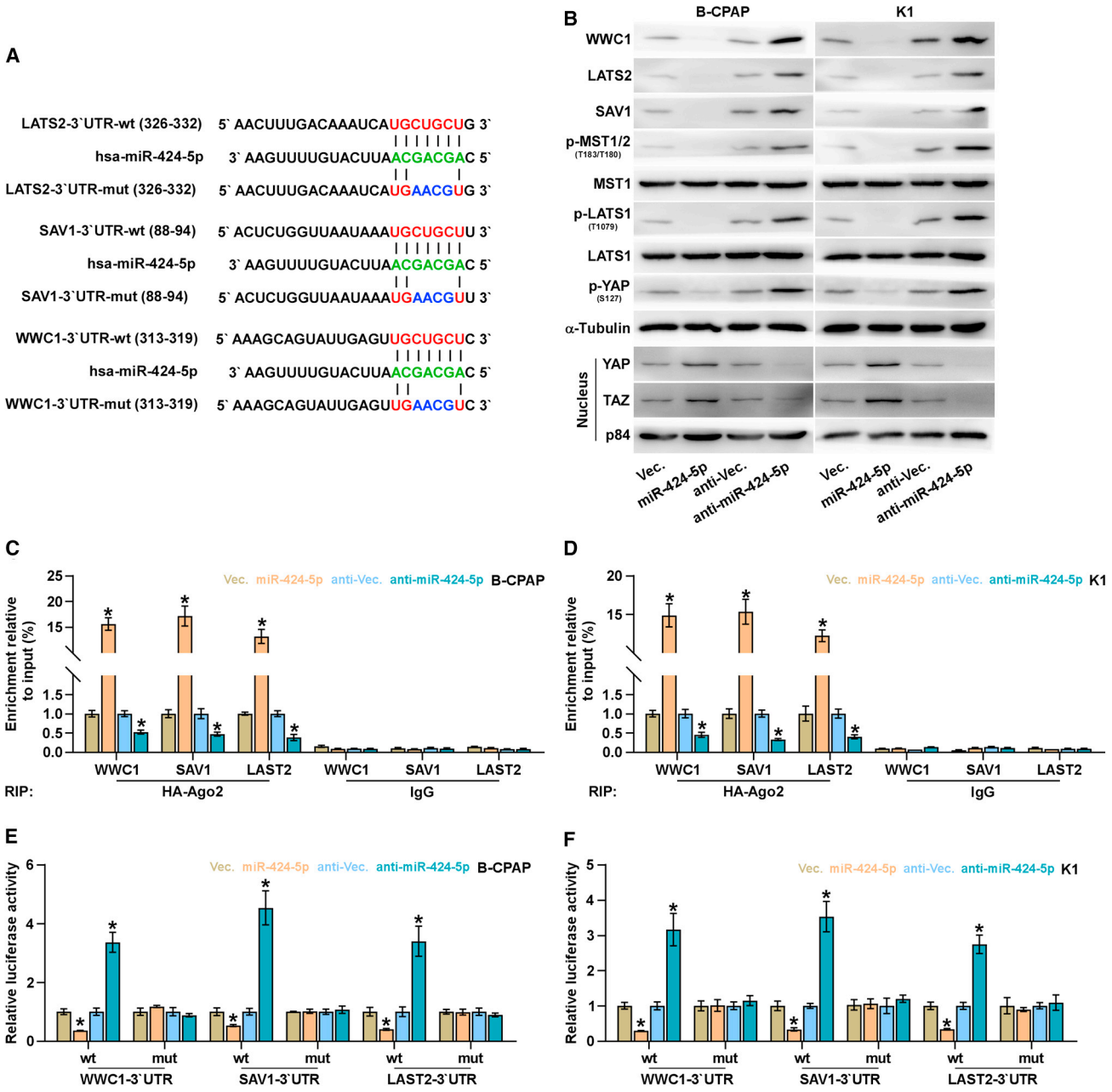

Figure 6. miR-424-5p Targets WWC1, SAV1, and LATS2

(A) Predicted miR-424-5p targeting sequence and mutant sequences in 3′ UTRs of WWC1, SAV1, and LATS2. (B) Western blot analysis of WWC1, SAV1, LATS2, p-MST1/2, MST1, p-LATS1, LATS1, p-YAP, YAP, and TAZ expression in the indicated cells. α-Tubulin and p84 were used as total and nuclear loading controls, respectively. (C and D) microribonucleoprotein (miRNP) IP assay showing the association between miR-424-5p, and WWC1, SAV1, and LATS2 transcripts in B-CPAP (C) and K1 (D) cells. Pulldown of IgG antibody served as the negative control. Each bar represents the mean values ± SD of three independent experiments.(E and F) Luciferase assay of cells transfected with pmirGLO-3′ UTR reporter of WWC1, SAV1, and LATS2 in the miR-424-5p-overexpressing and -silencing B-CPAP (E) and K1 (F) cells. Each bar represents the mean values ± SD of three independent experiments. *$p < 0.05$.

reduced. Furthermore, miR-424-5p expression was dramatically up-regulated in the tumor tissues of the mice inoculated with K1 cells stably transfected with pri-miR-424 compared with those in the vector at the end of the experiments; conversely, WWC1, SAV1 and LAST2, and YAP1 expression levels were robustly reduced (Figures S1C–S1F). The tumor tissues inoculated with miR-424-5p down-expressing K1 cells displayed an opposite expression pattern (Figures S1C–S1F). Taken together, miR-424-5p expression levels were

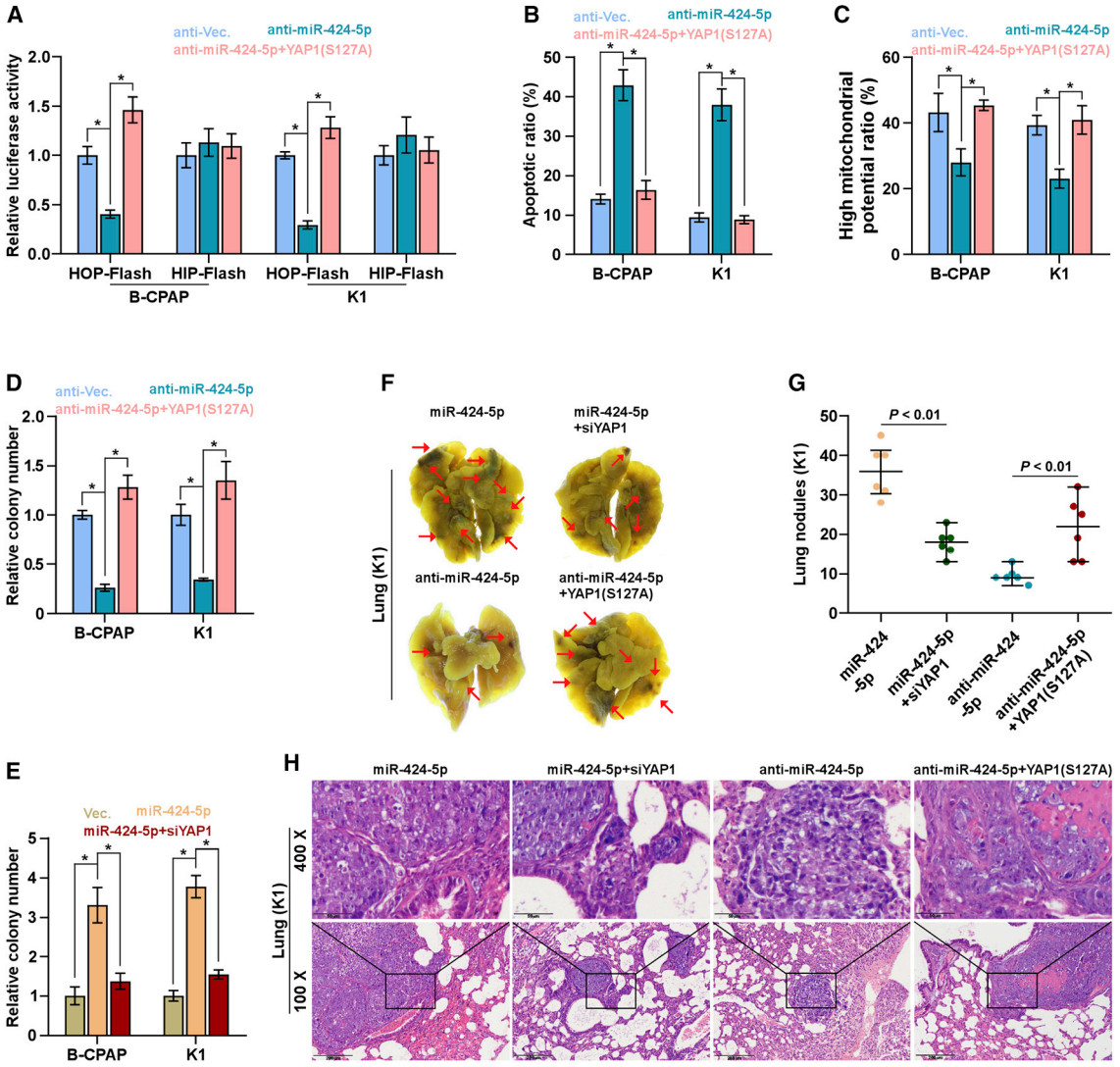

Figure 7. miR-424-5p Promotes Anoikis Resistance via Inactivating Hippo Signaling

(A) YAP1-S127A reversed the TEAD transcriptional activity repressed by downregulation of miR-424-5p assessed by HOP-Flash luciferase reporter. Each bar represents the mean values ± SD of three independent experiments. *p < 0.05. (B) YAP1-S127A reversed the pro-apoptotic role of miR-424-5p downregulation on thyroid cancer cells. Each bar represents the mean values ± SD of three independent experiments. *p < 0.05. (C and D) YAP1-S127A reversed the inhibitory effects of miR-424-5p downregulation on mitochondrial potential (C) and anchorage-independent growth capability (D) in thyroid cancer cells. Each bar represents the mean values ± SD of three independent experiments. *p < 0.05. (E) Silencing YAP1 attenuated the stimulatory effects of miR-424-5p overexpression on colony formation capability in thyroid cancer cells. Each bar represents the mean values ± SD of three independent experiments. *p < 0.05. (F) Representative images of the lung metastases formed from the indicated cells in the mice (n = 6, each group). (G) The numbers of lung tumor nests in each group were counted under a low-power field and are presented as the median values ± quartile values. *p < 0.05. Each bar represents the median values ± quartile values. (H) Representative H&E staining images of lung metastasis nodules in the indicated mouse groups. Scale bars, 200 μm (original magnification ×100); 50 μm (original magnification ×400).

negatively correlated with WWC1, SAV1 and LAST2, and YAP1 expression in thyroid cancer.

DISCUSSION

In this study, our results revealed overexpression of miR-424-5p in thyroid cancer tissues, which was significantly correlated with distant metastasis of thyroid cancer. Gain- and loss-of-function assays demonstrated that upregulating miR-424-5p promoted, whereas silencing miR-424-5p inhibited, anoikis resistance and lung metastasis of thyroid cancer cells *in vitro* and *in vivo*. Our results further showed that miR-424-5p promoted anoikis resistance and lung metastasis by inactivating Hippo signaling via simultaneously targeting WWC1, SAV1, and LAST2. Therefore, our findings elucidate a critical role of miR-424-5p in lung metastasis of thyroid cancer, as

well as unravel a novel mechanism underlying a pro-metastatic role of miR-424-5p in thyroid cancer.

A number of publications in literature have reported that miR-424-5p was upregulated in cutaneous squamous cell carcinoma,[26] gastric cancer,[27] and hepatocellular carcinoma,[28] which contributed to the tumorigenesis and metastasis in these cancer types. Conversely, miR-424-5p was reduced in endometrial cancer,[37,38] and upregulation of miR-424-5p produced a repressive effect on proliferation, growth, invasion, migration, or radioresistance in these cancer cells.[37,39,40] These studies have indicated that miR-424-5p plays a paradoxical role in different types of cancer dependent on cellular context or functional relevance. Of note, overexpression of miR-424-5p was positively correlated with the metastasis of colorectal cancer.[41] Importantly, our previous study has reported that miR-424-5p overexpression has been identified to be associated with aggressive clinical features in thyroid cancer patients.[29] These findings supported the notion that miR-424-5p may play an important role in malignant progression or metastasis of cancers. In the current study, we found that miR-424-5p was upregulated in thyroid cancer, which predicted a high distant metastatic potential in thyroid cancer patients. In a lung metastasis model of mouse, our results found that upregulating miR-424-5p promoted, whereas silencing miR-424-5p inhibited, lung metastatic ability of thyroid cancer cells *in vivo*. Functional experiments further revealed that miR-424-5p promoted lung metastasis of thyroid cancer dependent on ability of anoikis resistance, but not on the proliferation ability. Further mechanistic investigation revealed that miR-424-5p promoted anoikis resistance and lung metastasis by inactivating Hippo signaling via directly targeting WWC1, SAV1, and LAST2. Therefore, our results determine an oncogenic role of miR-424-5p in lung metastasis of thyroid cancer depending on the resistance of thyroid cancer cells to anoikis.

Several lines of evidence have reported that loss or downregulation of the core kinase, such as MST1/2 or LATS1/2, contributed to inactivation of Hippo signaling. For example, heat shock protein 70-induced downregulation of LAST1 promoted cisplatin resistance in prostate cancer cells;[42] downexpression of SAV1 by hypermethylation promoted invasion and migration of pancreatic ductal adenocarcinoma cells via inactivating Hippo signaling;[43] and furthermore, inactivation of Hippo signaling by epigenetic silencing of the WWC1 promoted the tumorigenesis of breast cancer.[44] However, how these core kinases of Hippo signaling are simultaneously disrupted in cancers, which constitutively inactivates Hippo signaling, remains not clarified. In this study, our results revealed that miR-424-5p inactivated Hippo signaling via concomitantly targeting WWC1, SAV1, and LAST2, as demonstrated by the increased luciferase reporter activity of HOP-Flash; the decreased phosphorylated levels of MST1, LATS1, and YAP; the increased nuclear expression of YAP and TAZ; and the elevated expression levels of multiple downstream genes of the Hippo pathway in thyroid cancer cells. Therefore, our findings unravel a novel mechanism responsible for inactivation of Hippo signaling in thyroid cancer.

Several lines of evidence have demonstrated that cancer cells have the capacity to survive under suspension conditions, namely, anoikis resistance, which is a major hallmark of metastasis in cancer, greatly promoting the distant metastatic ability of cancer cells. Haemmerle et al.[30] have reported that platelet-induced resistance to anoikis is critical for liver metastasis of colon cancer cells *in vivo*; in addition, upregulation of miR-133a-3p attenuated anoikis resistance of prostate cancer cells and repressed bone metastasis of prostate cancer cells *in vivo*.[32] In this study, our results revealed that upregulating miR-424-5p promoted anoikis resistance *in vitro* and lung metastasis *in vivo*; conversely, silencing miR-424-5p improved anoikis resistance and repressed the lung metastasis ability of thyroid cancer cells. Furthermore, our results further demonstrated that gain or loss of miR-424-5p had no effect on the proliferation and growth of thyroid cancer cells *in vitro*. Therefore, our results implied that miR-424-5p promotes lung metastasis of thyroid cancer in an anoikis resistance-dependent and proliferation-independent manner.

In summary, our results indicate that miR-424-5p inhibits activity of Hippo signaling via targeting WWC1, SAV1, and LAST2, which further promotes lung metastasis of thyroid cancer. Therefore, our results present novel findings to improve our understanding of the molecular mechanisms underlying lung metastasis of thyroid cancer, which will provide novel visions into facilitating the development of anti-lung metastasis therapeutic strategies in thyroid cancer.

MATERIALS AND METHODS

Cell Lines and Cell Culture

The normal primary thyroid follicular epithelial (PTFE) cells and thyroid duct cell carcinoma cells TT were purchased from Procell, and all thyroid cancer cell lines, including papillary thyroid cancer (PTC) cell lines, B-CPAP and BHT101, and anaplastic thyroid cancer (ATC) cell lines, CAL-62 and 8305C, were obtained from Shanghai Chinese Academy of Sciences cell bank (China). PTFE cells were cultured in medium (CM-H023; Procell, China), and thyroid cancer cell lines were cultured in RPMI-1640 medium (Life Technologies, Carlsbad, CA, USA) supplemented with penicillin G (100 U/mL), streptomycin (100 mg/mL), and 10% fetal bovine serum (FBS; Life Technologies). All cell lines were cultured at 37°C in a humidified atmosphere with 5% CO_2.

Patients and Tumor Tissues

A total of 10 paired fresh thyroid cancer tissues with the matched adjacent normal tissues were obtained during surgery at the China-Japan Union Hospital of Jilin University (Changchun, China) between January 2017 and December 2018 (Table S1). Patients were diagnosed based on clinical and pathological evidence, and the specimens were immediately snap frozen and stored in liquid nitrogen tanks. For the use of these clinical materials for research purposes, prior patients' consents and approval from the Institutional Research Ethics Committee were obtained.

RNA Extraction, Reverse Transcription, and Real-Time PCR

RNA from tissues and cells was extracted (TRIzol; Life Technologies) according to the manufacturer's instructions. mRNA, long noncoding

RNA (lncRNA), and miRNA were reverse transcribed from the total RNA using the Revert Aid First Strand cDNA Synthesis Kit (Thermo, USA) according to the manufacturer's protocol. cDNA was amplified and quantified on ABI 7500HT system (Applied Biosystems, Foster City, CA, USA) using SYBR Green I (Applied Biosystems). The primers used in the reactions are listed in Table S2. Primers for miR-424-5p were synthesized and purified by RiboBio (Guangzhou, China). U6 or glyceraldehyde-3-phosphate dehydrogenase (GAPDH) was used as endogenous controls for miRNA or mRNA, respectively. Real-time PCR was performed, and relative fold expressions were calculated with the comparative threshold cycle ($2^{-\Delta\Delta Ct}$) method as described previously.[45]

Plasmid and Transfection

The human miR-424-5p gene was PCR amplified from genomic DNA and cloned into a pMSCV-puro retroviral vector (Clontech, Japan). Pathway Profiling System, including pAP1-luc, pCRE-luc, pE2F-TA-luc, pERE-luc, pGRE-luc, pHSE-luc, pISRE-TA-luc, pMYC-luc, pNF-κB-TA-luc, pp53-TA-luc, pSRE-luc, and pSTAT3-TA-luc, was purchased from Clontech (PT3286-1). HOPFlash (Catalog [Cat.] 83467), HIPFlash (Cat. 83466), TOPFlash (Cat. 12456), and FOPFlash (Cat. 12457) were purchased from Addgene. The 3′ UTRs of WWC1, SAV1, and LATS2 were PCR amplified from genomic DNA and cloned into pmirGLO vectors (Promega, USA), and the list of primers used in cloning reactions was provided in Table S3. Anti-miR-424-5p was synthesized and purified by GENECHEM (China). The primers of the mutant plasmid for WWC1, SAV1, and LAST2 were synthesized and purified by HDbio (Guangzhou, China). Transfection of plasmids was performed as previously described.[46]

Western Blotting Analysis

Western blot was performed according to a standard method, as described previously.[47] Antibodies against BAX, BAD, BCL2L1, BCL2, p-MST1/2, MST1, p-LATS1, LATS1, p-YAP, and YAP were purchased from Cell Signaling Technology, and TAZ from Abcam. The membranes were stripped and reprobed with an anti-α-tubulin antibody (Cell Signaling Technology) as the loading control.

Anchorage-Independent Growth Assay

Five hundred cells were trypsinized and resuspended in complete medium containing 0.3% agar (Sigma). This experiment was performed as previously described[48] and carried out three times independently for each cell line.

Cell Counting Kit-8 Analysis

A total of 2×10^3 cells were seeded into 96-well plates, and the specific staining process and methods were performed according to the previous study.[49]

Colony Formation Assay

The cells were trypsinized as single cell and suspended in the media with 10% FBS. The indicated cells (300 cells/well) were seeded into a six-well plate for ~10–14 days. Colonies were stained with 1% crystal violet for 10 min after fixation with 10% formaldehyde for 5 min. Plating efficiency was calculated as previously described.[50] Different colony morphologies were captured under a light microscope (Olympus).

Cell-Cycle Analysis

Pretreatment and staining was performed using Cell Cycle Detection Kit (KeyGEN, China) as previously described.[51] In brief, cells (5×10^5) were harvested by trypsinization, washed in ice-cold PBS, and fixed in 75% ice-cold ethanol in PBS. Before staining, cells were gently resuspended in cold PBS, and ribonuclease was added into the cell suspension tube incubated at 37°C for 30 min, followed by incubation with propidium iodide (PI) for 20 min at room temperature. Cell samples (2×10^4) were then analyzed by FACSCanto II flow cytometer (Becton, Dickinson and Company, Franklin Lakes, NJ, USA), and the data were analyzed using FlowJo 7.6 software (Tree Star, Ashland, OR, USA).

Anoikis Induction Assay

Cell culture plates were coated with poly-HEMA (P3932; Sigma-Aldrich, St. Louis, MO, USA), a non-adhesive substratum, and allowed to evaporate to dryness at room temperature. Cells were kept in suspension by using poly-HEMA-coated plates to prevent adhesion. After 48 h of suspension, cells were harvested for cell viability analysis by 3-(4,5-dimethyl-2-thiazolyl)-2,5-diphenyl-2-H-tetrazolium bromide (MTT) assay and cell apoptosis analysis by flow cytometry.

Flow Cytometric Analysis

Flow cytometric analyses of apoptosis were done using the Fluorescein Isothiocyanate (FITC) Annexin V Apoptosis Detection Kit I (BD, USA) and were performed as previously described.[52] The cell's inner mitochondrial membrane potential ($\Delta\psi m$) was detected by flow cytometry using MitoScreen JC-1 staining kit (BD) and was presented as a protocol as described. In brief, cells were dissociated with trypsin and resuspended at 1×10^6 cells/mL in assay buffer and then incubated at 37°C for 15 min with 10 μL/mL JC-1. Before analysis by flow cytometer, cells were washed twice by assay buffer. Flow cytometry data were analyzed using FlowJo 7.6 software (Tree Star, USA).

Caspase-9 or Caspase-3 Activity Assays

Activity of caspase-9 or caspase-3 was analyzed by spectrophotometry using Caspase-9 Colorimetric Assay Kit or Caspase-3 Colorimetric Assay Kit (Keygen, China), and the protocol was presented as described. In brief, 5×10^6 cells or 100 mg fresh tumor tissues was washed with cold PBS, resuspended in lysis buffer, and incubated on ice for 30 min; then mixed with the 50 μL cell suspension, 50 μL reaction buffer, and 5 μL caspase-3/-9 substrate; and then incubated at 37°C for 4 h. The absorbance was measured at 405 nm, and BCA protein quantitative analysis was used as the reference to normal in each experiment group.

Immunofluorescence

Immunofluorescence was conducted as previously described.[53] Primary antibodies against YAP (Cat. 14074; Cell Signaling Technology) and CytoPainter Phalloidin-iFluor 488 Reagent (Cat. ab176753;

Abcam) were used. After counterstaining with DAPI (Invitrogen), the slide was observed under a confocal microscope (Zeiss).

Tumor Xenografts

Four- to six-week-old BALB/c-nu mice were purchased from the Experimental Animal Center of the Guangzhou University of Chinese Medicine and housed as previously described.[54] The mice were randomly divided into three groups (n = 6 per group), and the indicated K1 cells (1×10^6) were injected into mice via tail vein. Lungs were fixed in formalin and embedded in paraffin using a routine method. H&E staining was performed on sections from paraffin-embedded samples for pathologic examination of lung nodules. The number of lung tumor nests in each group was counted under 10 random low-power fields (LPFs).

Luciferase Assay

Cells (4×10^4) were seeded in triplicate in 24-well plates and cultured for 24 h, and the luciferase reporter assay was performed as previously described.[55] Cells were transfected with 100 ng HOP-Flash (Cat. #83467; Addgene) or HIP-Flash luciferase reporter plasmid (Cat. #83466; Addgene), plus 5 ng pRL-TK Renilla plasmid (Promega) using Lipofectamine 3000 (Invitrogen) according to the manufacturer's recommendation. Luciferase and Renilla signals were measured 36 h after transfection using a Dual Luciferase Reporter Assay Kit (Promega) according to the manufacturer's protocol.

miRNA Immunoprecipitation

Cells were co-transfected with hemagglutinin (HA)-Ago2, followed by HA-Ago2 immunoprecipitation using anti-HA-antibody, as previously described.[51] Real-time PCR analysis of the IP material was performed to test the association of the mRNA of WWC1, SAV1, and LAST2 with the RNA-induced silencing complex (RISC) complex.

Statistical Analysis

All values are presented as means ± SD. Significant differences were determined using GraphPad 5.0 software (USA). Student's t test was used to determine statistical differences between two groups. One-way ANOVA was used to determine statistical differences between multiple testing. Survival curves were plotted using the Kaplan-Meier method and compared by log-rank test. $p < 0.05$ was considered significant. All the experiments were repeated three times.

SUPPLEMENTAL INFORMATION

Supplemental Information can be found online at https://doi.org/10.1016/j.omto.2019.10.008.

AUTHOR CONTRIBUTIONS

H.S. developed ideas and drafted the manuscript. X.L., Y.F., and G.Z. conducted the experiments and contributed to the analysis of data. D.Z., N.L., and F.L. contributed to the analysis of data. C.L. and C.S. conducted the experiments. J.J. and H.L. contributed to the analysis of data and revised the manuscript. Z.Z. and G.D. edited the manuscript. All authors contributed to revise the manuscript and approved the final version for publication.

CONFLICTS OF INTEREST

The authors declare no competing interests.

ACKNOWLEDGMENTS

We would like to thank Prof. Haixia Guan from the Department of Endocrinology Institute at the China Medical University for papillary thyroid cancer cell lines TPC-1 and K1. This study was supported by the National Natural Science Foundation of China (grant 81702652) and China Postdoctoral Science Foundation (grant 2017M621177).

REFERENCES

1. Blomberg, M., Feldt-Rasmussen, U., Andersen, K.K., and Kjaer, S.K. (2012). Thyroid cancer in Denmark 1943-2008, before and after iodine supplementation. Int. J. Cancer *131*, 2360–2366.
2. Albores-Saavedra, J., Henson, D.E., Glazer, E., and Schwartz, A.M. (2007). Changing patterns in the incidence and survival of thyroid cancer with follicular phenotype—papillary, follicular, and anaplastic: a morphological and epidemiological study. Endocr. Pathol. *18*, 1–7.
3. Hay, I.D., Thompson, G.B., Grant, C.S., Bergstralh, E.J., Dvorak, C.E., Gorman, C.A., Maurer, M.S., McIver, B., Mullan, B.P., Oberg, A.L., et al. (2002). Papillary thyroid carcinoma managed at the Mayo Clinic during six decades (1940-1999): temporal trends in initial therapy and long-term outcome in 2444 consecutively treated patients. World J. Surg. *26*, 879–885.
4. Lim, S.M., Shin, S.J., Chung, W.Y., Park, C.S., Nam, K.H., Kang, S.W., Keum, K.C., Kim, J.H., Cho, J.Y., Hong, Y.K., and Cho, B.C. (2012). Treatment outcome of patients with anaplastic thyroid cancer: a single center experience. Yonsei Med. J. *53*, 352–357.
5. Besic, N., and Gazic, B. (2013). Sites of metastases of anaplastic thyroid carcinoma: autopsy findings in 45 cases from a single institution. Thyroid *23*, 709–713.
6. Pan, D. (2010). The hippo signaling pathway in development and cancer. Dev. Cell *19*, 491–505.
7. Halder, G., and Johnson, R.L. (2011). Hippo signaling: growth control and beyond. Development *138*, 9–22.
8. Harvey, K.F., Zhang, X., and Thomas, D.M. (2013). The Hippo pathway and human cancer. Nat. Rev. Cancer *13*, 246–257.
9. Lei, Q.Y., Zhang, H., Zhao, B., Zha, Z.Y., Bai, F., Pei, X.H., Zhao, S., Xiong, Y., and Guan, K.L. (2008). TAZ promotes cell proliferation and epithelial-mesenchymal transition and is inhibited by the hippo pathway. Mol. Cell. Biol. *28*, 2426–2436.
10. Oka, T., Mazack, V., and Sudol, M. (2008). Mst2 and Lats kinases regulate apoptotic function of Yes kinase-associated protein (YAP). J. Biol. Chem. *283*, 27534–27546.
11. Zhang, H., Liu, C.Y., Zha, Z.Y., Zhao, B., Yao, J., Zhao, S., Xiong, Y., Lei, Q.Y., and Guan, K.L. (2009). TEAD transcription factors mediate the function of TAZ in cell growth and epithelial-mesenchymal transition. J. Biol. Chem. *284*, 13355–13362.
12. Wang, X., Sun, D., Tai, J., Chen, S., Yu, M., Ren, D., and Wang, L. (2018). TFAP2C promotes stemness and chemotherapeutic resistance in colorectal cancer via inactivating hippo signaling pathway. J. Exp. Clin. Cancer Res. *37*, 27.
13. Garcia-Rendueles, M.E., Ricarte-Filho, J.C., Untch, B.R., Landa, I., Knauf, J.A., Voza, F., Smith, V.E., Ganly, I., Taylor, B.S., Persaud, Y., et al. (2015). NF2 Loss Promotes Oncogenic RAS-Induced Thyroid Cancers via YAP-Dependent Transactivation of RAS Proteins and Sensitizes Them to MEK Inhibition. Cancer Discov. *5*, 1178–1193.
14. Liu, Z., Zeng, W., Maimaiti, Y., Ming, J., Guo, Y., Liu, Y., Liu, C., and Huang, T. (2019). High Expression of Yes-activated Protein-1 in Papillary Thyroid Carcinoma Correlates With Poor Prognosis. Appl. Immunohistochem. Mol. Morphol. *27*, 59–64.
15. Bartel, D.P. (2009). MicroRNAs: target recognition and regulatory functions. Cell *136*, 215–233.
16. Velu, V.K., Ramesh, R., and Srinivasan, A.R. (2012). Circulating MicroRNAs as Biomarkers in Health and Disease. J. Clin. Diagn. Res. *6*, 1791–1795.
17. Ren, D., Wang, M., Guo, W., Huang, S., Wang, Z., Zhao, X., Du, H., Song, L., and Peng, X. (2014). Double-negative feedback loop between ZEB2 and miR-145

regulates epithelial-mesenchymal transition and stem cell properties in prostate cancer cells. Cell Tissue Res. *358*, 763–778.

18. Jiang, C., Yu, M., Xie, X., Huang, G., Peng, Y., Ren, D., Lin, M., Liu, B., Liu, M., Wang, W., and Kuang, M. (2017). miR-217 targeting DKK1 promotes cancer stem cell properties via activation of the Wnt signaling pathway in hepatocellular carcinoma. Oncol. Rep. *38*, 2351–2359.
19. Guo, W., Ren, D., Chen, X., Tu, X., Huang, S., Wang, M., Song, L., Zou, X., and Peng, X. (2013). HEF1 promotes epithelial mesenchymal transition and bone invasion in prostate cancer under the regulation of microRNA-145. J. Cell. Biochem. *114*, 1606–1615.
20. Zhang, X., Ren, D., Wu, X., Lin, X., Ye, L., Lin, C., Wu, S., Zhu, J., Peng, X., and Song, L. (2018). miR-1266 Contributes to Pancreatic Cancer Progression and Chemoresistance by the STAT3 and NF-κB Signaling Pathways. Mol. Ther. Nucleic Acids *11*, 142–158.
21. Ren, D., Yang, Q., Dai, Y., Guo, W., Du, H., Song, L., and Peng, X. (2017). Oncogenic miR-210-3p promotes prostate cancer cell EMT and bone metastasis via NF-κB signaling pathway. Mol. Cancer *16*, 117.
22. Zhang, X., Liu, J., Zang, D., Wu, S., Liu, A., Zhu, J., Wu, G., Li, J., and Jiang, L. (2015). Upregulation of miR-572 transcriptionally suppresses SOCS1 and p21 and contributes to human ovarian cancer progression. Oncotarget *6*, 15180–15193.
23. Huang, S., Wa, Q., Pan, J., Peng, X., Ren, D., Huang, Y., Chen, X., and Tang, Y. (2017). Downregulation of miR-141-3p promotes bone metastasis via activating NF-κB signaling in prostate cancer. J. Exp. Clin. Cancer Res. *36*, 173.
24. Dai, Y., Wu, Z., Lang, C., Zhang, X., He, S., Yang, Q., Guo, W., Lai, Y., Du, H., Peng, X., and Ren, D. (2019). Copy number gain of ZEB1 mediates a double-negative feedback loop with miR-33a-5p that regulates EMT and bone metastasis of prostate cancer dependent on TGF-β signaling. Theranostics *9*, 6063–6079.
25. Pallante, P., Battista, S., Pierantoni, G.M., and Fusco, A. (2014). Deregulation of microRNA expression in thyroid neoplasias. Nat. Rev. Endocrinol. *10*, 88–101.
26. Mizrahi, A., Barzilai, A., Gur-Wahnon, D., Ben-Dov, I.Z., Glassberg, S., Meningher, T., Elharar, E., Masalha, M., Jacob-Hirsch, J., Tabibian-Keissar, H., et al. (2018). Alterations of microRNAs throughout the malignant evolution of cutaneous squamous cell carcinoma: the role of miR-497 in epithelial to mesenchymal transition of keratinocytes. Oncogene *37*, 218–230.
27. Wei, S., Li, Q., Li, Z., Wang, L., Zhang, L., and Xu, Z. (2017). Correction: miR-424-5p promotes proliferation of gastric cancer by targeting Smad3 through TGF-β signaling pathway. Oncotarget *8*, 34018.
28. Lu, M., Kong, X., Wang, H., Huang, G., Ye, C., and He, Z. (2017). A novel microRNAs expression signature for hepatocellular carcinoma diagnosis and prognosis. Oncotarget *8*, 8775–8784.
29. Cong, D., He, M., Chen, S., Liu, X., Liu, X., and Sun, H. (2015). Expression profiles of pivotal microRNAs and targets in thyroid papillary carcinoma: an analysis of The Cancer Genome Atlas. OncoTargets Ther. *8*, 2271–2277.
30. Haemmerle, M., Taylor, M.L., Gutschner, T., Pradeep, S., Cho, M.S., Sheng, J., Lyons, Y.M., Nagaraja, A.S., Dood, R.L., Wen, Y., et al. (2017). Platelets reduce anoikis and promote metastasis by activating YAP1 signaling. Nat. Commun. *8*, 310.
31. Buchheit, C.L., Weigel, K.J., and Schafer, Z.T. (2014). Cancer cell survival during detachment from the ECM: multiple barriers to tumour progression. Nat. Rev. Cancer *14*, 632–641.
32. Tang, Y., Pan, J., Huang, S., Peng, X., Zou, X., Luo, Y., Ren, D., Zhang, X., Li, R., He, P., and Wa, Q. (2018). Downregulation of miR-133a-3p promotes prostate cancer bone metastasis via activating PI3K/AKT signaling. J. Exp. Clin. Cancer Res. *37*, 160.
33. Agarwal, V., Bell, G.W., Nam, J.W., and Bartel, D.P. (2015). Predicting effective microRNA target sites in mammalian mRNAs. eLife *4*, e05005.
34. John, B., Enright, A.J., Aravin, A., Tuschl, T., Sander, C., and Marks, D.S. (2004). Human MicroRNA targets. PLoS Biol. *2*, e363.
35. Dweep, H., Sticht, C., Pandey, P., and Gretz, N. (2011). miRWalk—database: prediction of possible miRNA binding sites by "walking" the genes of three genomes. J. Biomed. Inform. *44*, 839–847.
36. Liu, J., Ye, L., Li, Q., Wu, X., Wang, B., Ouyang, Y., Yuan, Z., Li, J., and Lin, C. (2018). Synaptopodin-2 suppresses metastasis of triple-negative breast cancer via inhibition of YAP/TAZ activity. J. Pathol. *244*, 71–83.
37. Dong, P., Xiong, Y., Yue, J., Hanley, S.J.B., and Watari, H. (2018). miR-34a, miR-424 and miR-513 inhibit MMSET expression to repress endometrial cancer cell invasion and sphere formation. Oncotarget *9*, 23253–23263.
38. Lu, Z., Nian, Z., Jingjing, Z., Tao, L., and Quan, L. (2017). MicroRNA-424/E2F6 feedback loop modulates cell invasion, migration and EMT in endometrial carcinoma. Oncotarget *8*, 114281–114291.
39. Ruiz-Llorente, L., Ardila-González, S., Fanjul, L.F., Martínez-Iglesias, O., and Aranda, A. (2014). microRNAs 424 and 503 are mediators of the anti-proliferative and anti-invasive action of the thyroid hormone receptor beta. Oncotarget *5*, 2918–2933.
40. Wang, X., Li, Q., Jin, H., Zou, H., Xia, W., Dai, N., Dai, X.Y., Wang, D., Xu, C.X., and Qing, Y. (2016). miR-424 acts as a tumor radiosensitizer by targeting aprataxin in cervical cancer. Oncotarget *7*, 77508–77515.
41. Torres, S., Garcia-Palmero, I., Bartolomé, R.A., Fernandez-Aceñero, M.J., Molina, E., Calviño, E., Segura, M.F., and Casal, J.I. (2017). Combined miRNA profiling and proteomics demonstrates that different miRNAs target a common set of proteins to promote colorectal cancer metastasis. J. Pathol. *242*, 39–51.
42. Ren, A., Yan, G., You, B., and Sun, J. (2008). Down-regulation of mammalian sterile 20-like kinase 1 by heat shock protein 70 mediates cisplatin resistance in prostate cancer cells. Cancer Res. *68*, 2266–2274.
43. Wang, L., Wang, M., Hu, C., Li, P., Qiao, Y., Xia, Y., Liu, L., and Jiang, X. (2017). Protein salvador homolog 1 acts as a tumor suppressor and is modulated by hypermethylation in pancreatic ductal adenocarcinoma. Oncotarget *8*, 62953–62961.
44. Liu, X., Li, C., Zhang, R., Xiao, W., Niu, X., Ye, X., Li, Z., Guo, Y., Tan, J., and Li, Y. (2018). The EZH2- H3K27me3-DNMT1 complex orchestrates epigenetic silencing of the wwc1 gene, a Hippo/YAP pathway upstream effector, in breast cancer epithelial cells. Cell. Signal. *51*, 243–256.
45. Dai, Y., Ren, D., Yang, Q., Cui, Y., Guo, W., Lai, Y., Du, H., Lin, C., Li, J., Song, L., and Peng, X. (2017). The TGF-β signalling negative regulator PICK1 represses prostate cancer metastasis to bone. Br. J. Cancer *117*, 685–694.
46. Wu, N., Ren, D., Li, S., Ma, W., Hu, S., Jin, Y., and Xiao, S. (2018). RCC2 over-expression in tumor cells alters apoptosis and drug sensitivity by regulating Rac1 activation. BMC Cancer *18*, 67.
47. Ren, D., Wang, M., Guo, W., Zhao, X., Tu, X., Huang, S., Zou, X., and Peng, X. (2013). Wild-type p53 suppresses the epithelial-mesenchymal transition and stemness in PC-3 prostate cancer cells by modulating miR-145. Int. J. Oncol. *42*, 1473–1481.
48. Zhang, X., Zhang, L., Lin, B., Chai, X., Li, R., Liao, Y., Deng, X., Liu, Q., Yang, W., Cai, Y., et al. (2017). Phospholipid Phosphatase 4 promotes proliferation and tumorigenesis, and activates Ca^{2+}-permeable Cationic Channel in lung carcinoma cells. Mol. Cancer *16*, 147.
49. Zhang, X., Ren, D., Guo, L., Wang, L., Wu, S., Lin, C., Ye, L., Zhu, J., Li, J., Song, L., et al. (2017). Thymosin beta 10 is a key regulator of tumorigenesis and metastasis and a novel serum marker in breast cancer. Breast Cancer Res. *19*, 15.
50. Wang, M., Ren, D., Guo, W., Huang, S., Wang, Z., Li, Q., Du, H., Song, L., and Peng, X. (2016). N-cadherin promotes epithelial-mesenchymal transition and cancer stem cell-like traits via ErbB signaling in prostate cancer cells. Int. J. Oncol. *48*, 595–606.
51. Li, X., Liu, F., Lin, B., Luo, H., Liu, M., Wu, J., Li, C., Li, R., Zhang, X., Zhou, K., and Ren, D. (2017). miR-150 inhibits proliferation and tumorigenicity via retarding G1/S phase transition in nasopharyngeal carcinoma. Int. J. Oncol. *50*, 1097–1108.
52. Ren, D., Lin, B., Zhang, X., Peng, Y., Ye, Z., Ma, Y., Liang, Y., Cao, L., Li, X., Li, R., et al. (2017). Maintenance of cancer stemness by miR-196b-5p contributes to chemoresistance of colorectal cancer cells via activating STAT3 signaling pathway. Oncotarget *8*, 49807–49823.
53. Zhou, Y., He, X., Chen, Y., Huang, Y., Wu, L., and He, J. (2015). Exendin-4 attenuates cardiac hypertrophy via AMPK/mTOR signaling pathway activation. Biochem. Biophys. Res. Commun. *468*, 394–399.
54. Ma, Y., Huang, H., Jiang, J., Wu, L., Lin, C., Tang, A., Dai, G., He, J., and Chen, Y. (2016). AVE 0991 attenuates cardiac hypertrophy through reducing oxidative stress. Biochem. Biophys. Res. Commun. *474*, 621–625.
55. Ren, D., Dai, Y., Yang, Q., Zhang, X., Guo, W., Ye, L., Huang, S., Chen, X., Lai, Y., Du, H., et al. (2019). Wnt5a induces and maintains prostate cancer cells dormancy in bone. J. Exp. Med. *216*, 428–449.